

# A Multi-object Double Spectrograph for the Large Binocular Telescope

P. S. Osmer, B. Atwood, P. L. Byard, D. L. DePoy, T. P. O'Brien, R. W. Pogge, D. Weinberg  
Department of Astronomy, The Ohio State University

## ABSTRACT

We are building a Multi-Object Double Spectrograph for the Large Binocular Telescope. The main themes of our planned research with the instrument are the formation and evolution of galaxies and their nuclei and the evolution of large-scale structure in the universe, although we expect that the spectrograph will be used for many other varieties of programs as well. The science goals for the instrument dictate that it have the highest possible throughput from 320 to 1000 nm, spectral resolutions of  $10^3$  to  $10^4$ , and multi-object capability over an  $\sim 6'$  field. Our design is highly modular, so future upgrades (e.g., additional cameras, new gratings, and integral field units) should be straightforward.

**Keywords:** Optical spectrographs, large telescopes

## 1. INTRODUCTION

The Large Binocular Telescope (LBT) project is a partnership of the University of Arizona, the German LBTB consortium (MPIA, lead institute), the Italian astronomical community (through Arcetri Observatory), the Ohio State University, and the Research Corporation to build the world's largest telescope on a single mount. The telescope construction is progressing well and first light is expected in 2003. The initial instrument complement of the telescope will include a near-infrared camera/spectrograph (see Mandel et al. and Thatte et al. in these proceedings), a wide field optical imager (see Ragazzoni et al. in these proceedings), some interferometric capability (e.g. Hinz et al. in these proceedings), and an optical spectrograph. As part of our commitment to the project, we are building the optical spectrograph, which will be a facility instrument for all the LBT community. The primary science driver for the instrument for our group is a set of observational programs designed to address several key research topics on the evolution of galaxies and structure in the Universe. We plan to devote a significant fraction of our LBT observing time to these programs, the ultimate outcome of which should be major advances in our understanding of galaxy evolution. Our LBT partners will use the instrument for a wide variety of other research programs as well.

## 2. RESEARCH PROGRAM

Recent increases in the aperture and image quality of ground-based optical telescopes and the sensitivity of their instruments have greatly enhanced their power as cosmic time machines, capable of studying the populations of objects present when the universe was a small fraction of its current age. Unraveling cosmic history by studying the properties of faint, highly redshifted sources and the absorption by intervening material is one of the most compelling challenges for observational astronomy in the next decade. The OSU astronomy department will have a 1/6 share of observing time on the Large Binocular Telescope (LBT). During the first five years of LBT operation, the department plans to devote a substantial fraction (more than 50%) of its observing time to spectroscopic surveys aimed at understanding the formation and evolution of galaxies and active galactic nuclei and the evolution of large scale structure. Furthermore, since the spectrograph will serve as the LBT facility optical spectrograph, the instrument should see extensive service with the other LBT partners for a wide variety of research programs.

There are numerous open questions that our observations will address. What is the cosmic history of star formation and chemical enrichment? What physical processes determine this history? When did galaxies of different luminosities and morphologies assemble most of their mass into coherent units? What is the relation between galaxies observed at high redshift and galaxies in the universe today? What are the relations between the populations of high-z quasars, low-z AGNs, and supermassive black holes in local galaxies? What is the typical lifetime of luminous quasars? What mechanisms trigger quasar activity, and what physics drives the turn-on and turn-off of the quasar population? What are the relations between the diverse populations of objects by which we trace the evolution of structure in the universe: galaxies, quasars, damped Ly $\alpha$  systems, Lyman limit systems, and low column density Ly $\alpha$  forest absorbers? How does the structure traced by these populations relate to the structure in the underlying distribution of dark matter?

The last few years have seen major observational advances in these areas, including redshift surveys of flux-limited samples that probe the galaxy distribution out to  $z \approx 1$  (e.g., Lilly et al. 1995, Lin et al. 1999), HST studies of the morphological evolution of galaxies over this redshift range (e.g., Abraham et al. 1996), and “demographic” studies of the population of supermassive black holes in nearby galaxies (e.g., Magorrian et al. 1998, van der Marel 1999). Most dramatic has been the discovery of a large population of “normal” star-forming galaxies at  $z > 3$ , through a combination of multi-color selection of “Lyman-break” candidates and spectroscopic confirmation with the LRIS spectrograph on Keck (e.g., Steidel et al. 1996, Lowenthal et al. 1997). More recently, this population has also been probed with Ly $\alpha$  emission-line surveys (e.g., Hu et al. 1998), and discoveries of distant galaxies and quasars are now reaching to  $z = 5$  and beyond (Weymann et al. 1998, Spinrad et al. 1998, Chen et al. 1999, and Fan et al. 1999). These developments have made possible the first serious attempts at one of the major objectives of observational cosmology: a determination of the global history of star formation in the universe (e.g., Madau et al. 1996, Madau 1997, and Steidel et al. 1999). However, this determination suffers from many uncertainties, such as the poorly constrained contribution from low-luminosity systems and the possibility, supported by some studies of faint sub-millimeter sources (e.g., Blain et al. 1999), that a large fraction of the star formation occurs in regions enshrouded by dust. Even the basic properties of the Lyman-break objects at  $z \approx 3$  are a matter of debate. Some argue that these UV-luminous objects are massive systems forming stars at a fairly steady rate (e.g., Steidel et al. 1996), and others that they are small systems whose UV emission has been temporarily boosted by sudden bursts of star formation (e.g., Sawicki & Yee 1998, Kolatt et al. 1999). These disparate points of view have radically different implications for the place of Lyman-break systems in the overall story of galaxy formation and evolution.

Alongside the observational breakthroughs have come major advances in the theoretical framework for describing galaxy formation and evolution, with increasing sophistication of semi-analytic models (e.g., Kauffmann et al. 1993; Cole et al. 1994; Somerville & Primack 1999) and hydrodynamic numerical simulations (e.g., Navarro & Steinmetz 1997; Weinberg et al. 1997 and references therein). In contrast to the traditional picture in which galaxies maintain their identity and evolve largely in isolation, theoretical studies of hierarchical galaxy formation suggest that mergers and radical morphological transformations are a common feature of galaxy evolution, and that many of a galaxy’s stars form in sub-units that only later assemble into the galaxy itself. Recent analytic models have begun to explore the connection between the formation of galaxies and the onset and eventual decline of quasar activity (e.g., Haehnelt et al. 1998). Perhaps the most revolutionary theoretical transformation has been the new understanding of the low column density Ly $\alpha$  forest that has emerged from hydrodynamic cosmological simulations (e.g., Cen et al. 1994; Zhang et al. 1995, Hernquist et al. 1996, Miralda-Escudé et al. 1996) and related analytic models (e.g., Bi & Davidsen 1997, Hui et al. 1997). These investigations imply that there is a tight and physically straightforward correlation between observable Ly $\alpha$  optical depth and underlying dark matter density. They also imply that the statistical properties of absorption in Ly $\alpha$  forest spectra with resolution  $R \approx 2000-8000$  can provide powerful constraints on cosmological models and on the structure of the dark matter distribution (see, e.g., Croft et al. 1999, Nusser & Haehnelt 1999, Weinberg et al. 1999a).

We plan to pursue three linked observing programs that would lead to major advances in the understanding of cosmic structure formation and the evolution of the galaxy and quasar populations:

1. A spectroscopic survey of galaxies with  $z < 1$
2. A spectroscopic survey of galaxies and quasars with  $1 < z < 7$
3. A multiple-tracer study of structure evolution focused on the redshift range  $z \approx 1.7-4$

The last of these programs is the most observationally challenging and the most novel, and we believe that it will ultimately prove the most revealing. It is predicated on the idea that the clustering of a population of objects can reveal a great deal about the physics of their formation. This notion has already gained currency in the study of Lyman-break galaxy clustering (see, e.g., Adelberger et al. 1998, Katz et al. 1999), but we believe that it has much broader applicability, and that it becomes especially powerful when one considers cross-correlations between different tracer populations as well as clustering of the populations on their own. We further expect that the instrument will have a long lifetime as the facility optical spectrograph on the LBT and, hence, needs to satisfy the future needs of the department and meet the science goals of our LBT partners.

These observational programs then define the required capabilities for the LBT optical spectrometer:

- High throughput, to take full advantage of the LBT’s aperture for studies of faint objects.
- A multi-slit mode is required for efficient operation of most aspects of these programs.

- Long-slit capability, for the fluorescent Ly $\alpha$  emission searches and detailed kinematic studies of selected objects from program (1).
- Wavelength coverage to the atmospheric cutoff at 320nm, to obtain maximum overlap of observable spectral features over the redshift range of program (1) and, more importantly, to allow detection of Ly $\alpha$  absorption and emission features down to  $z=1.65$  for programs (2) and (3). Because the background targets for absorption studies become fainter at higher redshifts, we will probably get our most detailed measurements of structure at the lowest redshifts where we can observe Ly $\alpha$ , and the observing time required for fluorescent emission detection rises steeply with increasing redshift (Gould & Weinberg 1996).
- Wavelength coverage to the CCD sensitivity cutoff at 1000nm, to allow Ly $\alpha$  detection to  $z\approx 7$  for program (2) and to maximize the accessibility of spectral diagnostics for programs (1) and (2), in particular allowing the detection of spectral features near 400nm rest wavelength out to  $z=1.5$ .
- Resolution  $R\approx 2000$  for identifications and redshifts of faint objects, moderate resolution studies of the Ly $\alpha$  forest, and detection of high column density absorption systems against faint background targets.
- Resolution  $R\approx 8000$  for chemical and kinematic studies of galaxies in program (1), higher resolution maps of the Ly $\alpha$  forest against the brighter background targets in program (3), measurements of neutral hydrogen column densities of DLA systems, and fluorescent Ly $\alpha$  emission searches matched to the expected width of typical features.
- Flexibility to upgrade in the future to make use of on-going technological innovations.

### 3. GENERAL DESCRIPTION OF THE INSTRUMENT

MODS is designed to work at the straight  $f/15$  Gregorian focus of each of the 8.4-m LBT primary mirrors. Our scientific interests dictate that MODS offer moderate spectral resolutions ( $10^3$ – $10^4$ ), wide wavelength coverage (320–1000nm), and the ability to observe extremely faint objects ( $\geq 25$  mag). These objectives require that the instrument have excellent throughput from the atmospheric cut-off in the ultraviolet to the practical sensitivity limit of CCDs in the far red. No single reflective or antireflective coating will work optimally over this wavelength range without sacrificing one extreme or the other. This has led us to adopt a double spectrograph design (like the Palomar DBSP; Oke & Gunn 1982) with separate blue- and red-optimized channels to maximize the throughput. To further improve the effective throughput, a multi-object capability over a field large enough to include many typical objects is also required. There is sufficient density of objects within an  $\sim 4'$  field of view to give considerable multiplex advantage with a multislit system. Given the unique configuration of the LBT, the most effective use of the full LBT collecting area is to employ two independent spectrographs, providing costs can be kept reasonable and CCDs capable of very low readout noise can be obtained. The typical seeing expected at the LBT is  $\sim 0.6''$  (similar to that currently obtained at the MMT, WIYN, and KPNO). Slit widths should also allow for the best anticipated conditions (i.e.  $\sim 0.3''$ ; active/adaptive optics are planned, and the LBT image error budget is  $0.34''$ ) and for worse-than-average conditions (i.e.  $\sim 1.2''$ ). Table 1 summarizes the baseline operating modes of MODS with  $0.6''$  slits.

Table 1: MODS Baseline Operating Modes

Mode	FWHM (4 pixel)	Resolution ( $\lambda/\Delta\lambda$ )	Total Range (nm)	Coverage per setting	Order
Blue LoRes	0.15 nm	3000 (450nm)	300–600	300 nm	1
Blue HiRes	0.075 nm	6000 (450nm)	300–600	150 nm	2
Blue Imaging	Filter		300–600	Filter	n/a
Red HiRes	0.1 nm	8000 (800nm)	500–1000	200 nm	1
Red LoRes	0.27 nm	3000 (800nm)	500–1000	400 nm	1
Red XD	0.1 nm	8000 (800nm)	500–1000	500 nm	4–7
Red Imaging	Filter		500–1000	Filter	n/a

MODS will have three baseline observing modes: *long-slit*, *multi-slit*, and *imaging*:

**Long-slit mode**, in which a single  $6'$  long slit provides continuous spatial coverage across one axis of the MODS field-of-view. Long slits are useful for point sources, especially faint objects where sky subtraction is critical, and for spatially extended objects with a definite axis of symmetry. A  $0.6''$  slit is matched to four pixels of the detector, but a wider slit can be used with no noise penalty by binning the detector.

**Multi-slit mode**, in which an aperture mask is used to define a series of precisely-located “slitlets” centered on objects falling within the MODS field of view. At a penalty of slightly reduced spectral coverage near the ends of the field along the

dispersion axis of the system, spectra can be obtained of objects distributed in 2 dimensions, effectively multiplying the throughput of the spectrograph by the number of slitlets used. For example, we could easily accommodate 48 slitlets 5" long across a 4' field. Consideration of adequate sky subtraction suggests that for the faintest objects, 10"-long slits (for ~24 slitlets) would be optimal. Multislit modes are features of all major spectrographs being designed for use by the current and coming generation of large telescopes (e.g., GMOS, DEIMOS, and FORS). For flexibility and simplicity of operation, the best option appears to be custom aperture plates machined on-site.

**Direct-Imaging mode**, in which the spectrograph is used without a slit mask and the grating is replaced by a flat mirror. In addition to applications requiring direct imaging *per se*, MODS ability to quickly switch between direct imaging and slit spectroscopic modes provides a foolproof method of precise target acquisition and placement on the slits or multislits. The faintest objects observed with the LBT will be much fainter than the night sky brightness, and direct imaging will be essential for target acquisition.

#### 4. DETAILS OF THE INSTRUMENT DESIGN

In this section we describe some of the details of the MODS design. These are primarily based on a recent optical design analysis and our experience with other instruments. Much of the first part of the project will be devoted to thorough investigations of all aspects of the spectrograph design and the comments in this section represent only our current conceptual view of the instrument. Note, however, that this design does follow our general philosophy of simplicity, modularity, and low cost.

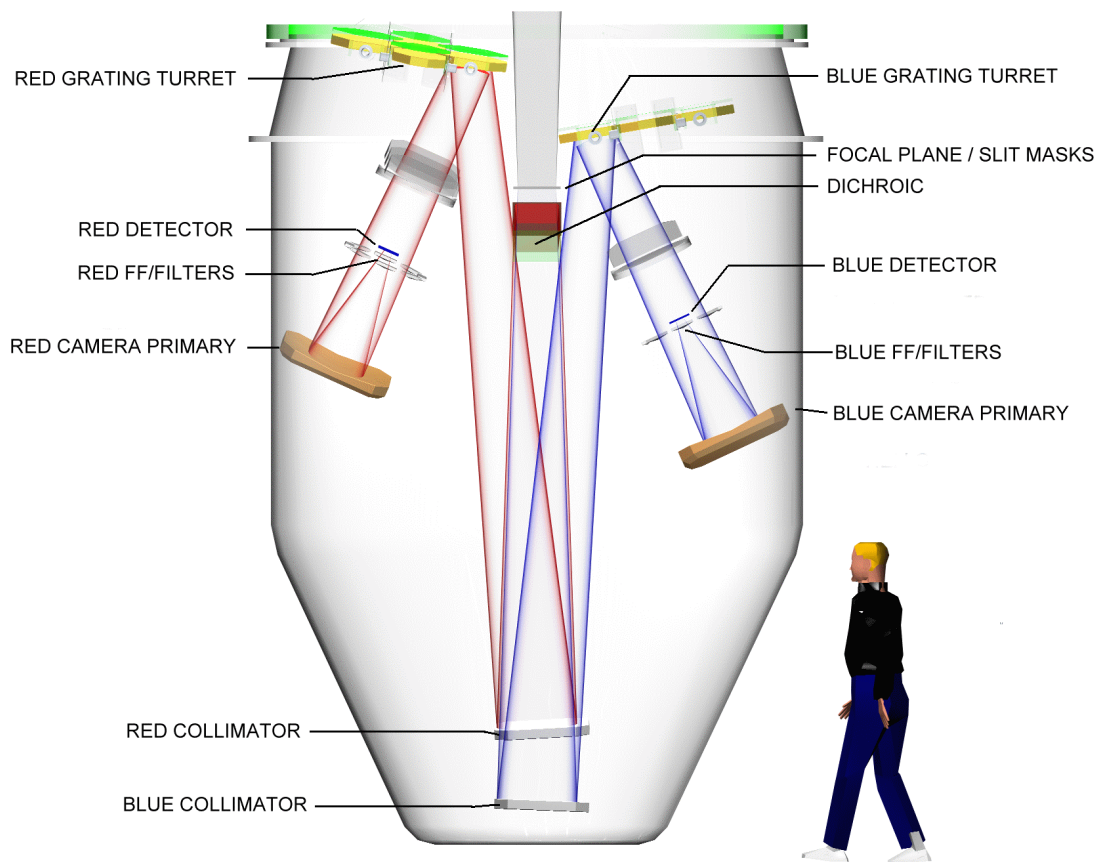


Figure 1 MODS Optical Layout

## Optical Design

The science goals for the instrument dictate that MODS must have high throughput from 320-1000nm, very good images over a 4° field and acceptable images over a larger 6° field, and resolutions of up to  $\sim 10^4$ . These requirements introduce important design constraints. For example, optical designs with many transmissive elements are likely to have marginal ultraviolet (or red) throughput due to the limitations of both the broad band coatings and the materials that have good transmission in the near UV.

We have adopted a design using a reflective collimator and a single-mirror camera with a correcting optic and field flattener as the best way to meet these requirements. Figure 1 shows a design which has been analyzed, meets the science requirements, but has not been fully optimized. The individual components of the design are discussed in more detail in the next section. Note that Figure 1 shows *all* of the optical surfaces in the spectrograph design. The large instrument volume available at the LBT allows for an instrument of this size (3.5×3.0-m) with only one reflection added for packaging.

**ADC:** An atmospheric dispersion compensation (ADC) assembly will be required when observing away from the zenith.

**Focal Plane:** The focal plane location is occupied either by a long slit, a mask with the desired slitlet pattern, or a field stop for imaging.

**Dichroic:** A dichroic beamsplitter reflects light of wavelength greater than 600nm to the red channel of the spectrograph and transmits light shortward of this wavelength to the blue channel. The dichroic can be removed under remote control to pass all of the light to the blue channel or replaced with a red-optimized mirror to pass all the light to the red channel. Our recent experience building an imaging instrument with similar split channels suggests that the light loss due to the dichroic will be less than 5%. The dichroic will have a transition from reflecting to transmitting over a wavelength of approximately 50nm allowing for enough overlap between red and blue spectra to simultaneously calibrate both channels. A flat dichroic would introduce some astigmatism in the blue channel. This astigmatism will be cancelled with a weak cylindrical figure on the rear surface of the dichroic substrate.

**Collimators:** Each channel will have decentered parabolic mirrors  $\sim 3.5$ -m from the  $f/15$  Gregorian focal plane that produce 230-mm diameter collimated beams. The large beam size has distinct advantages and comes at a relatively modest cost. The angular magnification at the camera aperture is the ratio of the telescope diameter to the point source collimated beam diameter. A larger beam reduces the camera field angle for a given field of view and mitigates important camera aberrations that increase very rapidly with the field angle. Since the optical power in the collimator and camera comes from reflective elements of relatively modest size, there is little cost difference between the required elements and ones half the size. An all-refractive collimator or camera with such a large beam, by contrast, would be prohibitively expensive.

**Gratings:** The angle between the camera and the collimator has been chosen to allow the spectrograph to operate at all required wavelengths and resolutions at reasonable grating angles. The grating size is consistent with commercially available large gratings and therefore permits the use of existing rulings or new rulings made with existing equipment and technology.

**Cross Disperser Grism (not labeled):** Cross dispersion in both channels will be with a removable grism. The grating portion of the grism will be ruled on an appropriate prism and will be of approximately 170 lines/mm to disperse the band perpendicular to the primary dispersion.

**Camera:** Identical cameras with 700mm focal length will be used in both channels that produce an image scale of 0.13" per 15 $\mu$ m pixel. The decentered Maksutov/Schmidt design gives good performance over the full range of incoming field angles and wavelengths. The camera has only two refractive elements and one reflection and the wavelength coverage of each camera will be less than an octave (allowing the use of high performance anti-reflection coatings on all air-glass surfaces), so the throughput should be very high. The cameras are large enough to accept the entire diffracted anamorphic beam from the gratings and the detectors do not obscure the dispersed beam, so there is zero vignetting. Furthermore, there is no narcissus effect, since light reflected from the detector escapes the system.

## Expected Performance

**Image Quality:** The analysis (using Code-V) of the collimator and camera combination shows that in direct imaging mode MODS will produce image sizes of  $<0.3''$  (80% encircled energy diameter) over a  $4'$  diameter field and  $<0.6''$  over a  $6'$  diameter field. This is sufficient to achieve the required science goals and obtain a significant multiplex advantage.

**Throughput:** The total throughput of the spectrograph is determined by the combination of the transmission and reflectance of the optical surfaces, the efficiency of the grating in use and the CCD quantum efficiency. Figure 2 shows the calculated throughput for the spectrograph and ADC based on published reflectivities for the mirrors, actual traces of anti-reflection coatings we have used on similar transmissive optics, measured detector quantum efficiency, and published grating blaze curves. We have not included slit losses or the efficiency of the primary and secondary in this calculation. Note that the throughput redward of 800nm would be significantly greater with a detector having a quantum efficiency similar to the thick fully-depleted demonstration devices made by LBNL/Lick.

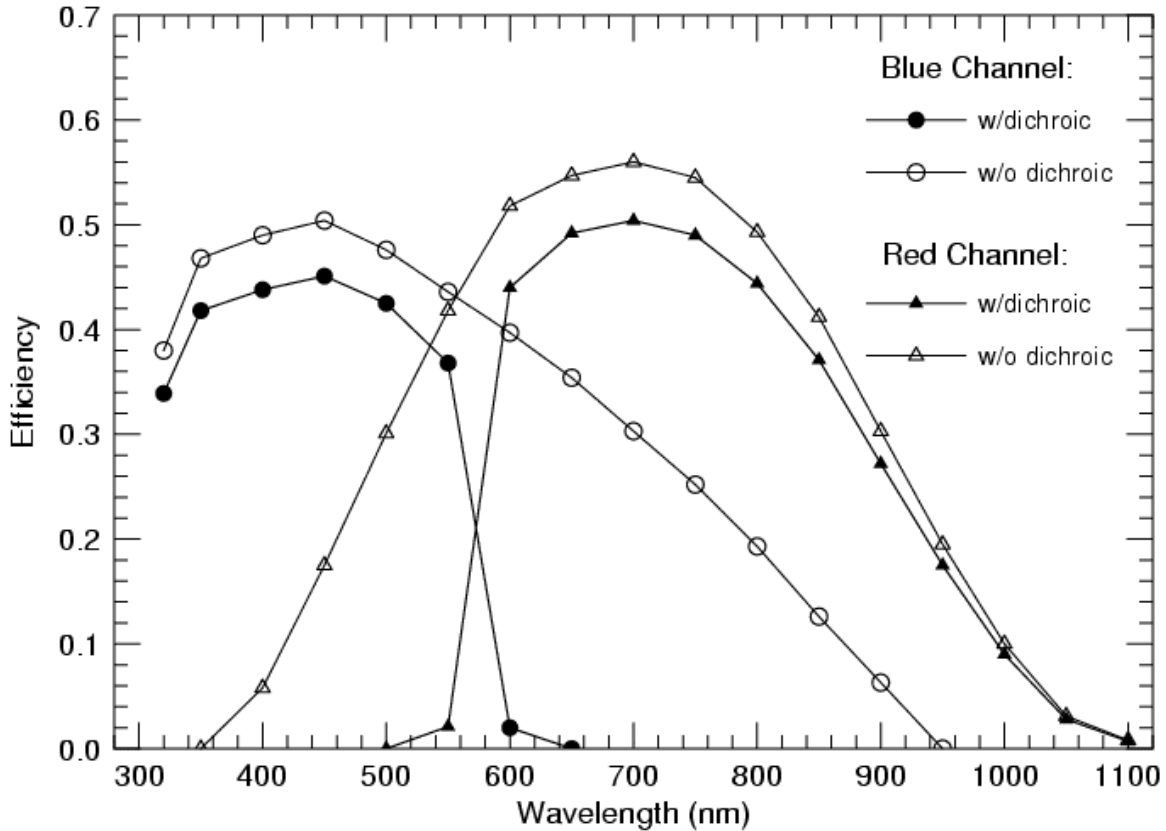


Figure 2: Expected MODS throughput excluding telescope and aperture

## Detectors

The design of MODS is predicated on the availability of very low readout noise CCDs. For example, if the readout noise is  $\leq 3 e^-$ , then the signal-to-noise ratio of digitally combined MODS observations are  $\leq 10\%$  less than single 11.8-m telescope measurements (assuming resolution  $\sim 10^4$ , slit  $\sim 0.6''$  wide, and dark sky conditions). Detector size, read-noise, cosmetics, and red quantum efficiency are all improving so rapidly that it would be unwise to commit to a given detector three years before an instrument is to be used. Nevertheless there are at least three sources of detectors that meet our basic requirements for format, low noise and high quantum efficiency. The SITe ST-002a, while not having the best noise or quantum efficiency, is commercially available. The MIT/Lincoln Labs CCID20 has excellent read noise, reasonable cosmetics, but has not demonstrated good blue quantum efficiency nor is its availability guaranteed. Devices with 4K $\times$ 2K format made from the Orbit Mask Set #1 have operated successfully and although they are not plentiful, it would be straightforward to make more devices with the same design, perhaps with a mask set having two or more copies of the device per wafer. We anticipate that devices from any of these sources would be thinned, packaged and coated by the Steward Observatory CCD Laboratory.

## Mechanical Design

The MODS spectrograph is a large structure to which modular components are attached. The structure supports the optical elements and mechanical modules against gravity loads. The configuration of the modules determines the instrumental mode. We have extensive experience in the design of precision automatic mechanisms for astronomical instruments. We have specified, designed, fabricated, and operated in the field devices such as filter wheels, slit wheels, camera interchange turrets, camera focus stages, pupil masks, and image rotators, all with excellent performance and reliability. Furthermore, we regularly use finite-element analysis techniques to design instruments that meet tight flexure and thermal stability requirements. The design of MODS will draw heavily from these previous efforts.

### *Structure Design*

The flexure design goal is to maintain image position on the detector to within 0.05 pixels ( $\sim 0.75\mu\text{m}$ ) for exposure times of roughly one hour in both the dispersion and slit directions. This insures that science programs requiring radial velocity resolution of a few  $\text{km s}^{-1}$  can be successful and that imaging performance will not be substantially degraded by flexure.

A welded steel frame will be designed to minimize translations and tilts of the optical elements, particularly the collimators. Welded steel construction is desirable because of its low hysteresis, high stability, moderately low coefficient of thermal expansion (CTE), low cost, and ease of fabrication. Careful interaction between the optical design (using CODE V) and the structural design (using ANSYS finite element analysis software) will insure that the structure is optimized for its optical support functions.

Preliminary analysis of a steel frame with the basic dimensions of the spectrograph indicates that collimator lateral translations of order  $25\mu\text{m}$  and collimator tilts of order  $5\mu\text{rad}$  can be expected from gravity induced flexure. The translation and tilt combine to produce image motion at the detector of approximately  $5\mu\text{m}$ . These results indicate that a simple uncompensated passive structure is unlikely to meet the image motion design requirement of  $0.75\mu\text{m}$ . Numerous flexure compensation techniques ranging from simple passive counter-balance systems to complex active optics with feedback are possible.

Our analysis indicates that a look-up table approach will provide a technically feasible, cost-effective solution for meeting the flexure requirements. The spectrograph will include 3 active linear actuators on the collimator support cells that will provide tip/tilt and focus movement of the collimator mirror. These actuators will be capable of tilting the collimator with the required precision to null flexure induced image motion to less than 0.05 pixels. The flexure induced image motion will be completely mapped, generating a look-up table that will provide the information necessary to drive the tip/tilt collimator. The success of a look-up table approach depends on a structural design with very low hysteresis, which is best provided by a welded steel frame. This flexure compensation approach is very similar to the pointing maps generated for large telescopes that routinely reduce their pointing errors by more than an order of magnitude.

Temperature gradients across the structure of  $1^\circ\text{C}$  will cause displacements in the structure of tens of microns, resulting in image motion at the detector of typically a few microns. To limit thermally induced image motion to less than  $0.75\mu\text{m}$ , changes in the temperature distribution across the structure must be less than a few tenths of a degree during an exposure. The entire instrument will be enclosed in an insulated cover which provides a homogeneous thermal environment and isolation from ambient temperature gradients in the dome and changing thermal radiation conditions. The hollow tubes of the structure will be actively ventilated by drawing air in through numerous small holes in the tube walls, minimizing

temperature gradients in the structure. This ventilation will also keep the structure very near ambient temperature eliminating any instrument seeing. The overall temperature of the structure will be monitored and a first order term for temperature compensation will be included in the lookup table to maintain collimator focus.

### *Module Design*

The spectrograph has six modules:

**ADC:** This mechanism will comprise two identical worm gears driven rotary motions with direct encoder feedback that will allow differential and common mode rotation of the ADC prisms.

**Slit-Mask Cassette:** Automatically selectable focal plane masks will be used for direct imaging single slit spectroscopy, and multi-slit spectroscopy. The masks must be fabricated and positioned in the instrument with high precision to insure registration between the focal plane mask and science field. Both GMOS (under construction for GEMINI) and DEIMOS (under construction for Keck) face similar challenges regarding focal plane masks. The GMOS design team has selected laser machining for fabrication of masks and a cassette mechanism for mask handling. The physical size of the GMOS masks and the slit widths are almost identical to our requirements because both instruments are used at  $f/15$  on 8-m telescopes. We plan to follow their progress carefully and to use the technologies and design approaches that best meet the needs of this instrument. This will substantially reduce costs and facilitate completion of this project.

The typical multi-slit observing session will obtain a direct image of the field of interest with the spectrograph direct imaging mode, either that night or using a queue scheduled service image obtained prior to the run. Targets are identified in this finder image, and the coordinates fed to a computer-controlled machine to generate the mask. Existing on-site mask generation systems can go from image to a ready-to-use mask in 30 minutes.

Design challenges for the multislit mode include developing an accurate mask delivery system that can be accessed easily by observing technicians, investigation of machining technologies that will deliver the necessary slit machining precision, structural requirements of the large aperture masks (including thermal expansion characteristics, stiffness against sag, distortions, etc.), and software for mask generation.

**Dichroic Changer:** A simple three position rotary drum will allow selection of either a red/blue dichroic when the spectrograph is used in a dual beam mode, a silver mirror to direct the beam into the red beam for red-only mode, or nothing when the operating in the straight-through blue-only mode.

**Collimator:** Each collimator cell will incorporate 3 linear actuators to allow remote tip/tilt and focus adjustments of the collimator. Stepper motor driven fine pitch screw actuators will provide the required resolution, accuracy, and stiffness for this application at moderate cost.

**Gratings:** Three gratings and one flat mirror will be mounted on a rotary indexer to permit quick reconfiguration of the instrument on the telescope. There will be a separate grating indexer for each beam accommodating a total of up to six gratings for the instrument. The gratings and flats will be mounted in kinematically docked cells. The grating indexer must be very accurate to insure that wavelength re-calibration will not be required after changing operating mode from imaging to spectroscopy. A grating tilt mechanism will be provided for each of the 3 grating positions to allow precise wavelength selection. The accuracy requirements for grating tilt are very demanding and the tilt mechanism will need to be very carefully developed.

**Cross-dispersing Grism:** The cross-dispersing grism will be kinematically mounted in a cell and removable from the grism select stage. A linear stage (perpendicular to the optical axis) will provide for up to 2 different grisms and one open position in the beam.

**Camera/Filter/Detector:** The Maksutov camera requires a simple plano-convex spherical field flattener immediately in front of the detector. This location is very desirable for filter placement, permitting the use of small and inexpensive filters. The MODS instrument will use field flatteners that carry a cemented rectangular filter on the flat side of the field flattener, providing the additional advantage of higher throughput by eliminating two air-to-glass surfaces and allowing optimized coatings on the convex surface of each flattener. The filter/flattener interchange mechanism will be a wheel capable of carrying ~8 filter/flattener combinations. We also anticipate including an unfiltered flattener (with appropriate broad-band



coating) and another wheel that holds only filters, so as to increase the flexibility of imaging observations. The camera will be focused by moving the primary mirror of the camera. The mirror will be supported on 3 motorized linear actuators, identical to the collimator mirror support actuators. The synchronized motion of the three actuators will provide focus travel while the tip/tilt motions will be used to collimate the camera primary mirror. The detector module is entirely outside the optical beam of the camera. This unobstructed design allows for simple and rigid support of the detector module.

## 5. FUTURE UPGRADE POSSIBILITIES

The MODS open architecture includes provisions for a number of future upgrades that would enhance the capabilities of the instrument and respond to the evolving scientific needs of its user community. A simple upgrade is to add more gratings to provide other resolution and wavelength coverage modes. Costs depend on the availability of replica gratings meeting the specifications. The modular design of the instrument would also allow for the implementation of new dispersing technologies such as Volume Phase Holographic gratings (Barden, Arns, & Colburn 1999; see also <http://www.noao.edu/ets/vpgratings>). These transmission-style dispersers could, for example, replace the cross-dispersing grisms in the collimated beam.

An especially powerful upgrade for MODS is to implement an integral-field mode. Not all astronomical objects have axes of symmetry that are convenient for deployment of a slit to measure their spectra. This is especially true of complex extended objects like active galactic nuclei, actively star-forming galaxies at high redshift, or individual HII regions in relatively nearby galaxies. An effective technique is to re-map the spatial field with arrays of fibers or microlenses and feed it to a long-slit spectrograph. Called integral field spectroscopy (IFS), this technique has been increasingly applied at a number of observatories for the study of angularly small extended objects (e.g., TIGER and MOS/ARGUS at CFHT [Bacon 1995; Vanderreist 1995]; HEXAFLEX and 2D-FIS at La Palma [Garcia et al. 1994]). There are several implementations of integral field that exist: packed fiber bundles, microlens arrays (Bacon 1995), and hybrids joining the two (e.g., Allington-Smith et al. 1996 for GMOS). The GMOS design is especially pertinent because of the similarities with the MODS optical requirements. We plan to study the alternatives and ensure that MODS will be able to include this capability in the future.

In summary, we are building a high-throughput optical spectrograph for LBT. We are designing the instrument to fulfill a specific set of scientific objectives, but expect that the spectrograph will see substantial use for a wide variety of projects both by us and our LBT partners. The instrument will have a long lifetime and we believe our modular approach will allow significant capability upgrades in the future.

## 6. REFERENCES

- Abraham, R. G., Tanvir, N. R., Santiago, B. X., Ellis, R. G., Glazebrook, K., & Van Den Bergh, S. 1996, MNRAS, 279, L47
- Adelberger, K. L., Steidel, C. C., Giavalisco, M., Dickinson, M., Pettini, M., & Kellogg, M. 1998, ApJ, 505, 18
- Allington-Smith, J., Content, R., Haynes, R., & Lewis, I. 1996, SPIE preprint.
- Bacon, R., et al. 1995, A&AS, 113, 347.
- Bacon, R., 1995, in *3D Optical Spectroscopic Methods in Astronomy*, G. Comte, M. Marcelin, eds., ASP Conf. Ser. 71, 239
- Barden, S., Arns, J., & Colburn, J. 1999, Proc SPIE 3749, 52 (see also <http://www.noao.edu/ets/vpgratings>)
- Bi, H.G., & Davidsen, A. 1997, ApJ, 479, 523
- Blain, A. W., Smail, I., Ivison, R. J., & Kneib, J.-P. 1999, MNRAS, 302, 632
- Bunker, A. J., Marleau, F. R., & Graham, J. R. 1998, AJ, 116, 2086
- Cen, R., Miralda-Escudé, J., Ostriker, J.P., & Rauch, M. 1994, ApJ, 437, L9
- Chen, H.-W., Lanzetta, K. M., & Pascarelle, S. 1999, Nature, 398, 586
- Cole, S., Aragon-Salamanca, A., Frenk, C. S., Navarro, J. F., & Zepf, S. E. 1994, MNRAS, 271, 781
- Croft, R. A. C., Weinberg, D. H., Pettini, M., Katz, N., & Hernquist, L. 1999, ApJ, 520, 1
- Dobrzycki, A., & Bechtold, J. 1991, ApJ, 377, L69
- Fan, X., et al. 1999, AJ, 118, 1
- Gallego, J., Zamorano, J., Aragon-Salamanca, A., & Rego, M. 1995, ApJ, 455, L1
- Gould, A., & Weinberg, D. H. 1996, ApJ, 468, 462
- Haehnelt, M. G., Natarajan, P., & Rees, M. J. 1998, MNRAS, 300, 817

- Hernquist L., Katz, N., Weinberg, D. H., & Miralda-Escudé, J. 1996, ApJ, 457, L5
- Hogan, C. J. & Weymann, R. J. 1987, MNRAS, 225, L1
- Hu, E. M., Cowie, L. L., & McMahon, R. G. 1998, ApJ, 502, L99
- Hui, L., Gnedin, N., & Zhang, Y. 1997, ApJ, 486, 599
- Jannuzi, B T. & Dey, A. 1999 in *Photometric Redshifts and High Redshift Galaxies*, eds. R. Weymann, L. Storrie-Lombard, M. Sawicki, & R. Brunner, ASP Conference Series, San Francisco, in press
- Kaiser, N. 1984, ApJ, 294, L9
- Katz, N., Hernquist, L., & Weinberg, D. H. 1999, ApJ, in press, astro-ph/9806257
- Kauffmann, G., White, S. D. M., & Guideroni, B. 1993, MNRAS, 264, 201
- Kolatt, T. S., et al. 1999, ApJ, submitted, astro-ph/9906104
- Lilly, S. J., LeFevre, O., Crampton, D. Hammer, F., & Tresse, L. 1995, ApJ, 455, 50
- Lilly, S. J., LeFevre, O., Hammer, F., & Crampton, D. 1996, ApJ, 460, L1
- Lin, H., Yee, H. K. C., Carlberg, R. G., Morris, S. L., Sawicki, M., Patton, D. R., Wirth, G., Shepherd, C. W. 1999, ApJ, 518, 533
- Lowenthal, J. D., Koo, D. C., Guzman, R., Gallego, J., Phillips, A. C., Faber, S. M., Vogt, N. P., Illingworth, G. D., & Gronwall, C. 1997, ApJ, 481, 673
- Madau, P. 1997, in *The Hubble Deep Field*, eds. M. Livio, S. M. Fall, & P. Madau (Cambridge: Cambridge University Press)
- Madau, P., Ferguson, H. C., Dickinson, M. E., Giavalisco, M., Steidel, C. C., & Fruchter, A. 1996, MNRAS, 283, 1388
- Miralda-Escudé J., Cen R., Ostriker, J.P., & Rauch, M. 1996, ApJ, 471, 582
- Magorrian, J., et al. 1998, AJ, 115, 2285
- Navarro, J. F., & Steinmetz, M. 1997, ApJ, 478, 13
- Nusser, A., & Haehnelt, M. 1998, MNRAS, 303, 179
- Osmer, P.S. 1998, in *The Young Universe*, ASP Conf. Ser. 146, 1, eds. S. D'Odorico, A. Fontana, & E. Giallongo.
- Sawicki, M., & Yee, H. K. C. 1998, AJ, 115, 1329
- Somerville, R. S., & Primack, J. R. 1999, MNRAS, in press, astro-ph/9802268
- Spinrad, H., Stern, D., Bunker, A., Dey, A., Lanzetta, K., Yahil, A., Pascarelle, S., & Fernandez-Soto, A. 1998, AJ, 116, 2617
- Steidel, C., Adelberger, K., Giavalisco, M., Dickinson, M., & Pettini, M. 1999, ApJ, 519, 1
- Steidel, C. C., Giavalisco, M., Pettini, M., Dickinson, M., & Adelberger, K. L. 1996, ApJ, 462, L17
- Turnshek, D. A., Wolfe, A. M., Lanzetta, K. M., Briggs, F. H., Cohen, R. D., Foltz, C. B., Smith, H. E., Wilkes, B. J. 1989, ApJ, 344, 567
- van der Marel, R. P. 1999, AJ, 117, 744
- Weinberg, D. H., et al. 1999a, in *Evolution of Large Scale Structure: From Recombination to Garching*, eds. A.J. Banday et al., (Twin Press: Vledder NL), astro-ph/9810142
- Weinberg, D. H., Davé, R., Gardner, J. P., Hernquist, L., & Katz, N. 1999b, in *Photometric Redshifts and High Redshift Galaxies*, eds. R. Weymann, L. Storrie-Lombard, M. Sawicki, & R. Brunner, ASP Conference Series, San Francisco, in press
- Weinberg, D. H., Katz, N., & Hernquist, L. 1998, in *Origins*, C. E. Woodward, J. M. Shull, & H. Thronson, eds., ASP Conf. Ser. 121, astro-ph/9708213
- Weymann, R. J., Stern, D., Bunker, A., Spinrad, H., Chaffee, F. H., Thompson, R. I., & Storrie-Lombardi, L. J. 1998, ApJ, 505, L95
- Vanderreist, C. 1995, in *3D Optical Spectroscopic Methods in Astronomy*, G. Comte, M. Marcelin, eds., ASP Conf. Ser. 71, 209.
- Zhang, Y., Anninos, P., & Norman, M. L. 1995, ApJ, 453, L57